Chemical Reduction of 2,4,6-Tricyano-1,3,5-triazine and 1,3,5-Tricyanobenzene. Formation of Novel 4,4′,6,6′-Tetracyano-2,2′-bitriazine and Its Radical Anion[†]

Rico E. Del Sesto,[‡] Atta M. Arif,[‡] Juan J. Novoa,[§] Iwona Anusiewicz,[||] Piotr Skurski,[||]
Jack Simons,[‡] Brian C. Dunn,[‡] Edward M. Eyring,[‡] and Joel S. Miller*,[‡]

*Department of Chemistry, University of Utah, 315 S. 1400 E. RM 2124, Salt Lake City, Utah 84112-0850,
Department of Chemistry, University of Gdansk, 80-952 Gdansk, Poland, and the Department of Physical
Chemistry, University of Barcelona, Av. Diagonal, 647, E-08028, Barcelona, Spain*

jsmiller@chemistry.utah.edu

Received April 17, 2002

Chemical reduction of 2,4,6-tricyano-1,3,5-triazine, TCT, results in the formation of an unstable radical anion that undergoes immediate dimerization at a ring carbon to form $[C_{12}N_{12}]^{2-}$, $[TCT]_2^{2-}$, characterized by a long 1.570 (4) Å central C−C bond. $[TCT]_2^{2-}$ can decompose into the radical anion of 4,4′,6,6′-tetracyano-2,2′-bitriazine, $[TCBT]^{•-}$, the one-electron reduced form of planar (D_{2h}) TCBT, which is also structurally characterized as the [TMPD][TCBT] charge-transfer complex (TMPD = N,N,N,N-tetramethyl-p-phenylenediamine) with a 1.492 (2) Å central $sp^2−sp^2$ C−C bond. Although crystals could not be obtained for the radical anion $[TCBT]^{•-}$, the electrochemistry ($E° = +0.03$ V), EPR ($g = 2.003$, $^2A_{^{14}N} = 3.347$ G, and $^4A_{^{14}N} = 0.765$ G and a line width of 0.24 G), and theoretical calculations support the formation of $[TCBT]^{•-}$. In addition, thermolysis of $[TCT]_2^{2-}$ yields $[TCBT]^{•-}$. Chemical reduction of 2,4,6-tricyanobenzene, TCB, forms an unstable radical anion that immediately undergoes dimerization at a ring carbon to form $[C_{12}H_6N_6]^{2-}$, $[TCB]_2^{2-}$, which has a long 1.560 (5) Å central C−C bond. Reaction of TCT with tetrathiafulvalene (TTF) forms structurally characterized [TTF][TCT], and in the presence of water, TCT hydrolyzes to 2,4-dicyano-6-hydroxy-s-triazine, DCTOH. In contrast, the reaction of TCT with TMPD forms [TMPD][TCT], which in the presence of water forms structurally characterized $[HTMPD]^+[DCTO]^-$.

Introduction

The broad class of substituted s-triazines are important in electronic and polymeric materials[1] in areas of organic and catalysis chemistry.[2] Essentially all 2,4,6-subsituted s-triazines substituted thus far have electron-releasing/-donating groups, e.g., amino, alkyl, aryl, alkoxy/aryloxy, and halides. Electron-withdrawing groups are not common because the resonance of the triazine ring localizes the electrons more on the nitrogens than on the carbons;

thus, substitution on the ring carbons with electron-withdrawing groups results in molecules that are extremely sensitive to nucleophilic substitution, particularly hydrolysis in the presence of even trace atmospheric water.[3,4]

2,4,6-Tricyano-1,3,5-triazine, TCT, is a particularly interesting as it is nitrogen-rich[5] and a trimer of cyanogen and an interesting new acceptor for the development of molecule-based magnets and conductors. In this regard, TCT forms a charge-transfer complex with tetrathiafulvalene (TTF), which after exposure to air exhibits relatively high dc electrical conductivity.[6] Furthermore, as a cyanocarbon, the nitriles can coordinate to metals and

[†] Dedicated to Prof. Mortimer M. Labes for his pioneering work in the area of azacarbon chemistry.

[‡] University of Utah.

[§] University of Barcelona.

[||] University of Gdansk.

(1) (a) Chang, Y.; Kim, Y. N.; Noh, I.; Kim, C. *Macromol. Chem. Phys.* **2000**, *201*, 1802. (b) Fink, R.; Heischkel, Y.; Thelakkat, M.; Schmidt, H.-W.; Jonda, C.; Hüppauff, M. *Chem. Mater.* **1998**, *10*, 3620. (c) Fink, R.; Frenz, C.; Thelakkat, M.; Schmidt., H.-W. *Macromolecules* **1997**, *30*, 8177.

(2) (a) Forbes, D. C.; Barrett, E. J.; Lewis, D. L.; Smith, M. C. *Tetrahedron Lett.* **2000**, 9943. (b) Venkataraman, K.; Wagle, D. R. *Tetrahedron Lett.* **1979**, 3037.

(3) (a) Smolin, E. M.; Rapoport, L. *The Chemistry of Heterocyclic Compounds: s-Triazines and Derivatives*; Interscience Publishers: New York, 1959; Vol. 13. (b) Quirke, J. M. E. *Comprehensive Heterocyclic Chemistry*, **1984**, *3*, 457 and references cited therein.

(4) Quirke, J. M. E. *Compr. Heterocycl. Chem.* **1984**, *3*, 457 and references cited therein.

(5) Subrayan, R. P.; Rasmussen, P. G. *Trends Polym. Sci.* **1995**, *3*, 165.

additionally give the molecule the capacity to accept electrons and become reduced to the radical anionic species.

TTF
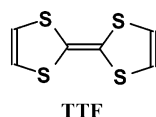
TCT has been reported to undergo an irreversible one-electron reduction with Na or K to form **1**•−.[7] The in situ-generated EPR spectra suggested two sets of equivalent nitrogen atoms in a 2:4 ratio, not by two sets of equivalent nitrogen atoms in a 3:3 ratio as expected for TCT•−. However, the number of bonds that need to be broken and created makes formation of **1**•−, via the reduction of TCT, dubious, which led to the possibility of a Jahn−Teller distortion of TCT•− as suggested by Carrington et al.[7]

TCT   **TCB**

1   **2**$^{2-}$
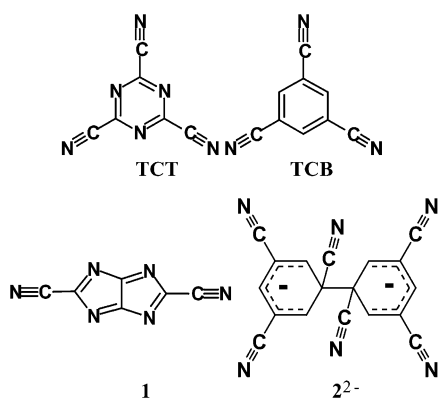
As our and previous groups' attempts to isolate any species via electrochemical methods failed,[7] we report herein the products that result from the chemical reduction of TCT and the structurally related 1,3,5-tricyanobenzene, TCB. The reductive dimerization of TCB was previously proposed to form **2**$^{2-}$.[8] Preliminary work in our laboratory,[9] however, revealed that **2**$^{2-}$ is not the reduction product of TCB. We also note that reduction of TCT also leads to the formation of redox-active 4,4′,6,6′-tetracyano-2,2′-bitriazine, TCBT, whose radical anion is the source of the EPR spectra previously reported for the product of the alkali metal reduction of TCT.
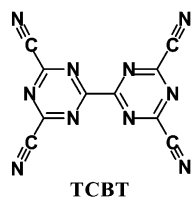
TCBT

Results and Discussion

Electrochemistry of TCT and TCB. The cyclic voltammogram (CV) of TCT, shows an irreversible reduc-

(6) Berlin, A.; Pagani, G. A.; Sannicolo, F. *Synth. Met.* **1987**, *19*, 415. (b) Berlin, A.; Pagani, G. A.; Sannicolo, F. *J. Chem. Soc., Chem. Commun.* **1986**, 1579.
(7) Carrington, A.; Longuet-Higgins, H. C.; Todd, P. F. *Mol. Phys.* **1965**, *9*, 211.
(8) Sertel, M.; Yildiz, A.; Gambert, R.; Baumgärten, H. *Electrochim. Acta* **1986**, *31*, 1287.
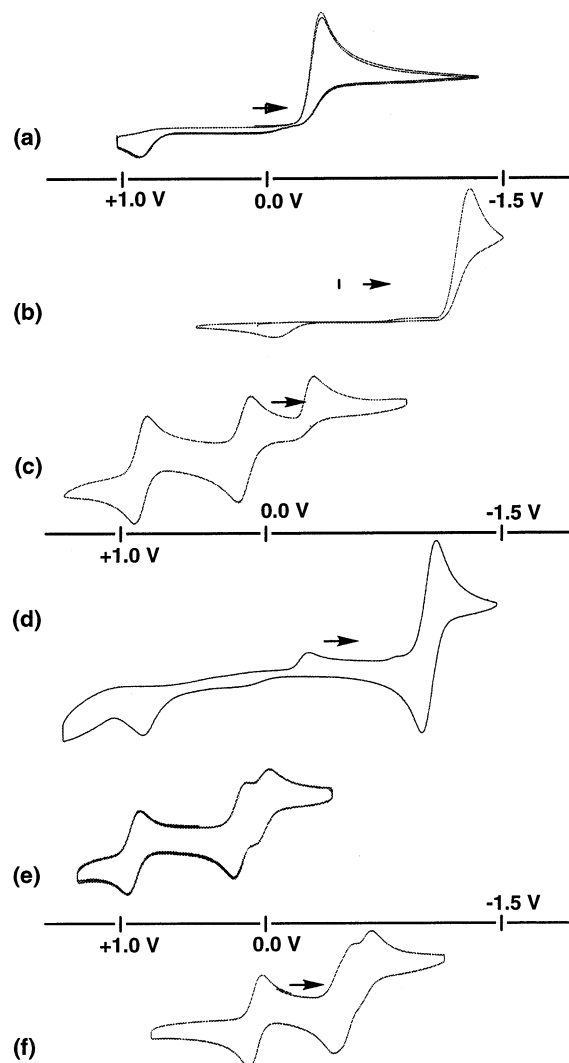(9) Del Sesto, R. E.; Arif, A. M.; Miller, J. S. *Chem. Commun.* **2001**, 2730.

FIGURE 1. Cyclic voltammograms at 100 mV/s in MeCN for (a) TCT, (b) TCB, (c) [TMPD][TCT], (d) {[Cr(mes)₂]⁺}₂[TCT]₂²⁻, (e) [TMPD][TCBT], and (f) [TDAE]²⁺{[TCBT]•−}₂.

tion at −0.39 V (vs SCE) and an irreversible oxidation at +0.70 V,[9] Figure 1a. Although TCT undergoes a one-electron reduction, it requires a much stronger reducing agent than typical cyanocarbon acceptors, e.g., TCNE and TCNQ.[10] The electrochemical behavior of TCB is analogous to that of TCT, but with an irreversible reduction at −1.35 V and an irreversible oxidation at −0.03 V (vs SCE), Figure 1b. Hence, TCB is 0.96 V more difficult to reduce than TCT. None of the voltammograms of TCT or TCB showed any sign of reversible behavior for either reductions or oxidations at scan rates of 5−2000 mV/s, suggesting that the irreversibility of the reduction may be due to a chemical reaction that is much faster than the electron-transfer process of the cyclic voltammetry.

Chemical Reactions and Reduction of TCT. To form charge-transfer complexes and electron-transfer salts, TCT was reacted with tetrathiafulvalene (TTF) ($E_{1/2}° = +0.30$ V vs SCE in MeCN),[10] *N,N,N,N*-tetramethyl-*p*-phenylenediamine (TMPD) ($E_{1/2}° = +0.10$ and 0.72 V),[11] bis(mesitylene)chromium(0), Cr(mes)₂ ($E_{1/2}° =$

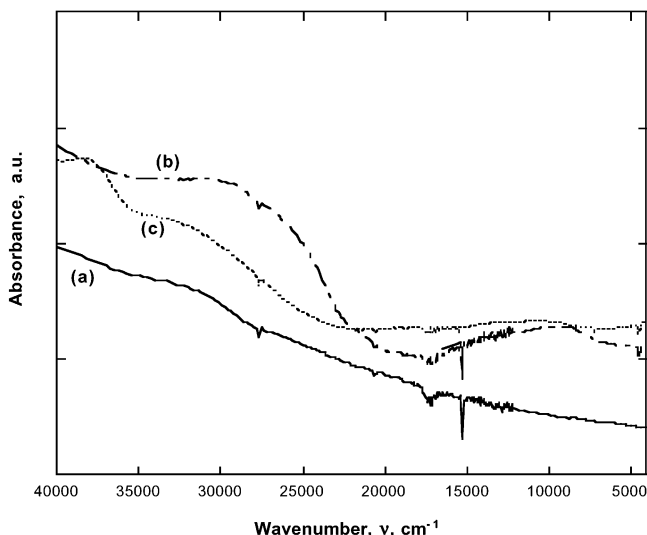(10) Ward, M. D. *Electroanal. Chem.* **1989**, *16*, 181.

FIGURE 2. Solid-state UV/visible/NIR spectra of (a) TTF°
(solid line) (b) [TTF][TCT] (dashed line), and (c) [TMPD][TCT]
(dotted line) as pressed KBr pellets.

−0.92 V),[12] Co^{II}Cp*$_2$ (Cp* = pentamethylcyclopentadi-
eneide) ($E_{1/2}°$ = −1.47 V),[13] and the two-electron donor
tetrakis(dimethylamino)ethylene, TDAE ($E_{1/2}°$ = −0.53
and −0.68 V).[14] The −0.39 V irreversible reduction
potential for TCT requires strong reducing agents for
electron transfer to occur and this is only expected for
the latter three electron donors.
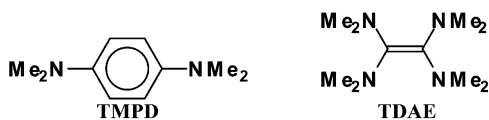
Reaction of TCT with TMPD. The reaction of TCT
with TMPD in MeCN leads to several products, including
[TMPD][TCT]. Although crystals suitable for the single-
crystal structural determination of [TMPD][TCT] were
not obtained, the electronic absorption spectrum of the
solid [TMPD][TCT] has an absorption at ∼10 000 cm^{-1}
(1000 nm), which is assigned to the TMPD → TCT charge
transfer (Figure 2a). Likewise, the IR spectrum shows
peaks predominantly from the two independent neutral
species. Hence, electron transfer does not occur in either
solution or in the solid state. This is confirmed as the
CV of [TMPD][TCT] shows the irreversible reduction of
TCT at −0.39 V in addition to the two one-electron
oxidations of TMPD (Figure 1c).

TMPD was reacted with TCT in MeCN containing ∼5%
water, and a yellow precipitate of [TMPD][DCTOH]
composition formed, whose structure was determined.
The single-crystal X-ray analysis shows that, as sug-
gested for [TTF][TCT],[6] the nucleophilic displacement of
one of the nitriles by water followed by a proton transfer

(acid−base reaction) from the resulting 2,4-dicyano-6-
hydroxy-*s*-triazine, DCTOH, to one of the TMPD nitro-
gens occurred. The presence of [HTMPD]$^+$ is based on
the twist of the dimethylamino group on N7 being 90°
out of the plane of the benzene ring, Figure 3, and the
average bond angle around N7 is 109.4°, indicating sp^3
hybridization. This is inconsistent with the expected
planarity of the TMPD molecule in its neutral state.
Though the proton position was refined as being bonded
to an sp^3-hybridized N7, it is expected that the 2,4-
dicyano-6-hydroxy-*s*-triazine would be fairly acidic con-
sidering the electronegativity of the triazine ring.[2,4,15]
The anionic charge in [DCTO]$^-$ is located within the ring,
and the resulting ketone is H-bonded to the [HTMPD]$^+$,
on the basis of the ring angle on N2 being 109.3° and
the angles around C1 averaging 120°. Hence, the struc-
ture is best described as [HTMPD]$^+$[DCTO]$^-$, Figure 3.
Calculations were carried out on [DCTO]$^-$ at the RHF/
6-31++G** level using the atomic coordinates from the
crystal structure of [HTMPD]$^+$[DCTO]$^-$. The calculations
show that the b$_1$ HOMO lies 10.737 eV below the a$_1$
LUMO, Figure 4, and the electron density principally
resides on the imide N, with respect to the O, Figure 4c,
Table 1.

[DCTO]$^-$
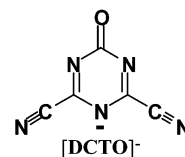
Reaction of TCT with TTF. TCT forms a charge-
transfer complex with tetrathiafulvalene, TTF.[6] Single-
crystal X-ray analysis shows that the structure of [TTF]-
[TCT] is comprised of stacks of alternating TTF and TCT
in a ···DADA··· (D = TTF; A = TCT) motif (Figure 5).[16]
The central C=C bond of the TTF fragment is 1.348 Å,
and inner C−S bonds are 1.756 Å. The [TTF][TCT] is
diamagnetic, and the bond lengths are comparable to
neutral TTF[17a] and other charge-transfer complexes of
TTF with C=C bond lengths of ∼1.35 Å and C−S bonds
lengths of ∼1.76 Å.[17] These bond lengths make the TTF^0
distinguishable from the radical cation and/or partially
charged TTF, which typically have C=C bonds of 1.404
Å and C−S bonds 1.713 Å, as seen in [TTF][ClO$_4$][17b] or
[TTF][SCN]$_{0.57}$.[17d] Hence, [TTF][TCT] is a charge transfer
complex and not an electron transfer salt, as initially
formulated but not structurally characterized.[6] The bulk
of the TCT ring overlaps with one ring of TTF. The closest
contact between the two moieties is 3.17 Å. The TTF and
TCT planes are not parallel within a stack, deviating by
∼8° from each other. The angle between the TTF in one
stack to TCT in an adjacent stack is ∼45°.

The UV/visible/NIR spectrum for the [TTF][TCT] in
MeCN is the sum of the solution spectra for TTF and

(11) Tanaka, S.; Bruce, J. A.; Wrighton, M. S. *J. Phys. Chem.* **1981**,
85, 3779.

(12) Yur'eva, L. P.; Peregudova, S. M.; Kravtsov, D. N.; Vasil'kov,
A. Yu.; Nekiasov, L. N.; Asfandiarov, N. L.; Timoshenko, M. M.; Chisov,
Yu. V. *J. Organomet. Chem.* **1987**, *336*, 371.

(13) Robbins, J. L.; Edelstein, N.; Spencer, B.; Smart, J. C. *J. Am.
Chem. Soc.* **1982**, *104*, 1882.

(14) Bock, H.; Borrmann, H.; Havlas, Z.; Oberhammer, H.; Ruppert,
K.; Simon, A. *Angew. Chem., Int. Ed.* **1991**, *30*, 1678.

(15) Wilmshurst, J. K. *J. Chem. Phys.* **1958**, *28*, 733.

(16) Del Sesto, R. E.; Botoshansky, M.; Kaftory, M.; Arif, A. M.;
Miller, J. S. *Cryst. Eng. Commun.* **2002**, *4*, 117.

(17) (a) Coppens, W. F.; Kenney, N. C.; Edmonds, J. C.; Nagel, A.;
Wudl, F.; Coppens, P. *Chem. Commun.* **1971**, 889. (b) Yakushi, K.;
Nishimura, S.; Sugano, T.; Kuroda, H. *Acta Crystallogr., Sect. B* **1980**,
36, 358. (c) Formigue, M.; Boubekeur, K.; Batail, P.; Renouard, J.;
Jacob, G. *New J. Chem.* **1998**, 845. (d) Formigue, M.; Boubekeur, K.;
Batail, P.; Renouard, J.; Jacob, G. *New J. Chem.* **1998**, 845. (e)
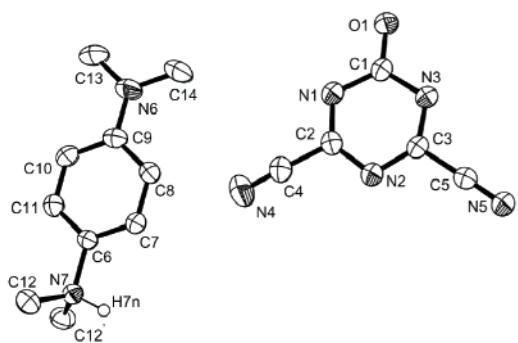Clemente, D. A.; Marzotto, A. *J. Mater. Chem.* **1996**, *6*, 941.

FIGURE 3. Structure of [HTMPD]⁺[DCTO]⁻. Bond angles around N6 range from 108.1(1)° for C6−N7−H7 to 112.44(11)° for C6−N7−C12. Bond lengths of the triazine ring are 1.242(3) Å for C1−O1, 1.383(3) for C1−N1, 1.319(3) Å for C1−N2, 1.337(3) Å for C2−N2, 1.337(3) Å for N2−C3, 1.310(3) Å for C3−N3, and 1.392(3) Å for N3−C1. Bond angle for N1−C1−N3 is 120.9(2)°, and that for C2−N2−C3 is 109.9(2)°.

FIGURE 5. Structure of [TTF][TCT] showing the overlap of TTF (light-colored spheres, with white as sulfur and gray as carbon atoms) and TCT rings (black spheres).
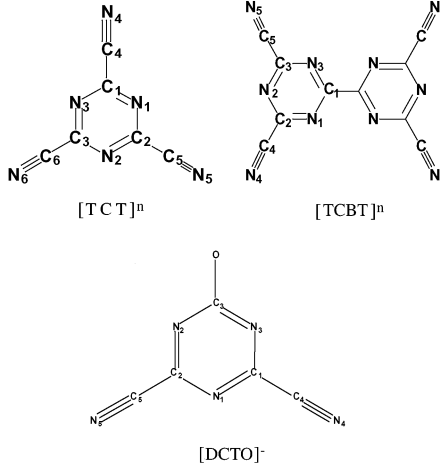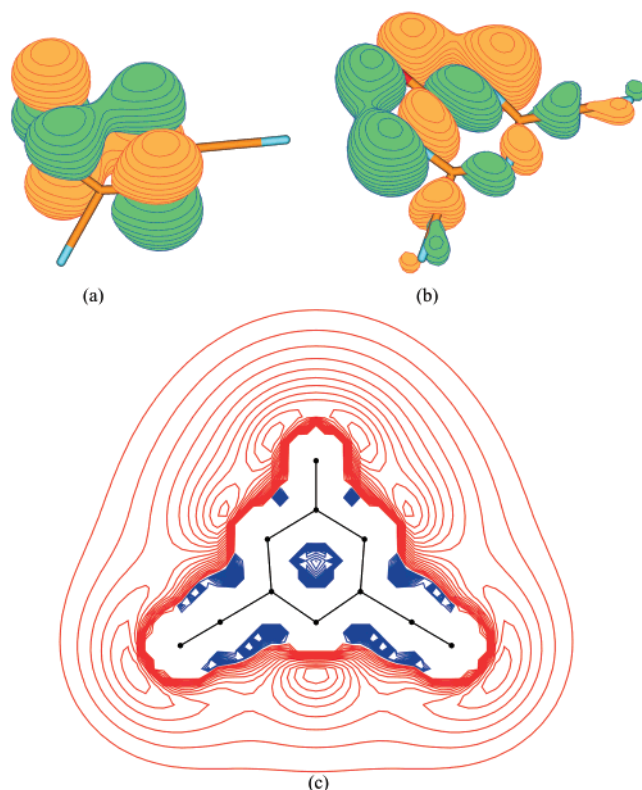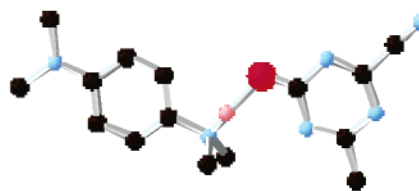

FIGURE 4. HOMO (a), LUMO (b), and calculated charge density (c) for [DCTO]⁻, where red and blue represent negative (−) and positive (+) potentials, respectively. Contour spacing for the orbitals is 0.03, and the electrostatic potential is 0.01250 e⁻.

TCT. However, in the solid state, as a pressed KBr pellet, a new absorption appears at 10 000 cm⁻¹ (1000 nm), which is assigned to a TTF → TCT charge transfer (CT) band as observed for [TMPD][TCT], Figure 2. The IR spectrum also shows peaks predominantly from the two independent neutral species, with slight shifts in the nitrile region of the TCT, as well as in the $v_{C\equiv N}$ (TCT) and v_{C-S} regions. Hence, electron transfer does not occur either in solution or in the solid state. This is consistent with the reported low dc electrical conductivity for [TTF]-[TCT].[6]

Upon exposure to the ambient laboratory atmosphere, [TTF][TCT] turns deep red forming a material that

exhibits significantly higher electrical conductivity ($\sigma \approx$ 0.5 S/cm).[6] Although unable to obtain a structure of the hydrolysis product of [TTF][TCT], on the basis of IR spectral changes, it was proposed that a nitrile on TCT is substituted by −OH from the water, with the loss of HCN, forming deep red [TTF][DCTOH][6] or, by analogy to the above reaction with TMPD, possibly [HTTF]⁺-[DCTO]⁻. The latter, however, is unlikely because the DCTOH v_{OH} absorption (∼3300 cm⁻¹) is observed in the IR spectrum of [TTF][DCTOH] but is absent in the [TMPD]⁺[DCTO]⁻. Since TTF is a poor proton acceptor and much less basic than TMPD,[18] proton transfer from this hydroxytriazine to TTF does not occur as it does for [TMPD][DCTOH]. The absence of proton transfer is also consistent with the absence of a shift in the absorptions of the IR of the TTF moiety, as well as the lack of a shift in the UV/visible absorption bands.

Reduction of TCT with Cr(mes)₂, CoCp*₂, and TDAE. The reaction of TCT with Cr(mes)₂ led to the formation of a product whose structure was determined to consist of the σ-dimer of [TCT]⁻, [C₁₂N₁₂]²⁻, [TCT]₂²⁻ (Figure 6a).[9] [TCT]₂²⁻ is a constitutional isomer of previously reported [C₁₂N₁₂]²⁻.[19] The structure of the [Cr-(mes)₂]₂[TCT]₂ has a 1.570 (4) Å σ-bond formed between two of the substituted triazine-ring carbons. Each triazine ring maintains its planarity, suggesting that the dimer-

(18) Attanasio, D.; Bonamico, M.; Fares, V.; Suber, L. *J. Chem. Soc., Dalton Trans.* **1992**, 2523.

(19) (a) Buschmann, W. E.; Arif, A. M.; Miller, J. S. *J. Chem. Soc., Chem. Commun.* **1995**, 2343. (b) Manson, J. L.; Buschmann, W. E.; Miller, J. S. *Inorg. Chem.* **2001**, *40*, 1926.

TABLE 1. Net Atomic Charges Obtained after a Mulliken Population Analysis of the Density Functional B3LYP/6-31++G(2d,2p) Wavefunction on Atoms of Neutral and Radical Anionic [TCT]^n and [TCBT]^n ($n = 0$, 1−)

molecule	atom	charge (e$^-$) $n = 0$	charge (e$^-$) $n = 1-$	spin (e$^-$) $n = 1-$
[TCT]^n	C1	0.921	0.914	−0.04
	C2, C3	0.921	0.924	0.26
	C4	−0.591	−0.634	0.00
	C5, C6	−0.591	−0.648	−0.04
	N1, N3	−0.112	−0.285	0.23
	N2	−0.112	−0.134	−0.10
	N4	−0.218	−0.337	−0.02
	N5, N6	−0.218	−0.395	0.13
[TCBT]^n	C1	−0.203	−0.212	0.314
	C2, C3	0.613	0.615	0.029
	N1, N3	−0.194	−0.244	0.121
	N2	−0.223	−0.301	0.033
	C4, C5	0.159	0.100	0.001
	N4, N5	−0.366	−0.466	0.003
[DCTO]$^-$	N1		−1.040	
	N2, N3		−1.052	
	N4, N5		−0.508	
	C1, C2		0.960	
	C3		1.415	
	C4, C5		0.312	
	O		−0.797	

ized carbons are predominantly of sp^2 character. Bond lengths within the triazine rings are 1.463(3) Å for C39−N2, 1.467(3) Å for C39−N3, 1.285(3) Å for C37−N3, 1.348(3) Å for C37−N1, 1.350(3) Å for C38−N1, and 1.289(3) Å for C38−N2. The IR spectrum for this salt exhibits peaks at ~1580, 1320, and 910 cm^{-1} as well as v_{CN} at 2242 cm^{-1}. The 1580 cm^{-1} peak is assigned to the ring C=N stretching mode that is blue shifted with respect to that observed for TCT due to the anionic charge residing within the ring.

Reaction of CoCp*$_2$ and TDAE with TCT leads to compounds of [CoCp*$_2$][TCT] and [TDAE][TCT]$_2$ composition, respectively. All three reduction products of TCT display characteristic peaks in the IR spectrum at 1580, 1320, and 910 cm^{-1}, and, hence, also possess [TCT]$_2^{2-}$.

The electrochemical behavior of all three salts of [TCT]$_2^{2-}$ is the same with an irreversible oxidation occurring at +0.70 V, Figure 1d, in addition to the reversible reductions of the cations. The irreversible oxidation is also seen in the CV of TCT, Figure 1a. This anodic peak is therefore attributed to the oxidation of
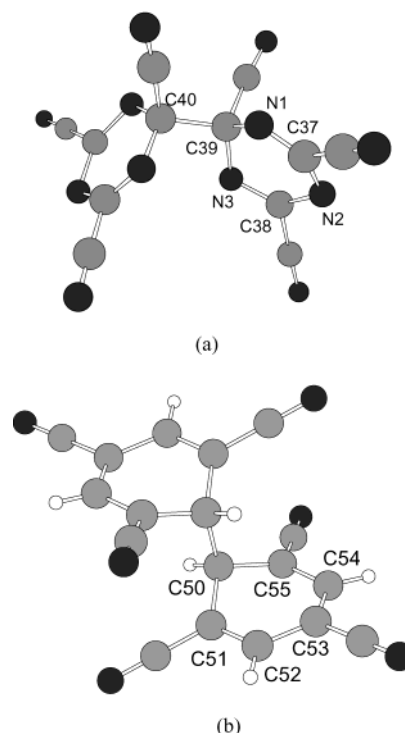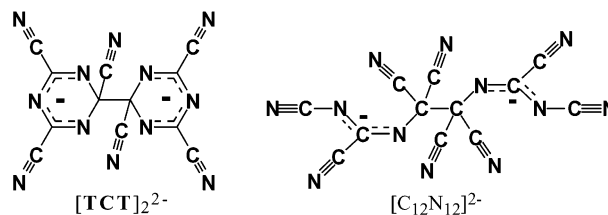
FIGURE 6. Structure of (a) [TCT]$_2^{2-}$ as observed in the [Cr-(mes)$_2$]$_2$[TCT]$_2$ s-dimer and (b) [TCB]$_2^{2-}$ as observed in [CoCp*$_2$]$_2$-[TCB]$_2$, with central dimer bonds of 1.570 (4) Å and 1.560 (5) Å, respectively. Lighter spheres are carbon, darker spheres nitrogen, and white spheres hydrogen.

[**TCT**]$_2^{2-}$ [C$_{12}$N$_{12}$]$^{2-}$

[TCT]$_2^{2-}$ to [TCT]$_2^{•-}$, which is unstable and breaks apart into [TCT]$^{•-}$ and TCT^0, Scheme 1. The irreversible reduction of TCT^0 can then be explained through the process of dimerization, and suggests that the radical anion [TCT]$^{•-}$ is not stable in the solvents used (MeCN, CH$_2$Cl$_2$, THF) and immediately dimerizes to [TCT]$_2^{2-}$, Scheme 1.

Reaction of TCB with CoCp*$_2$. Given the structural similarity of TCB with TCT and that the reduction of TCB was postulated to form **2**$^{2-}$ with a framework similar to [TCT]$_2^{2-}$,[8] we tried to isolate the TCB reduction product. The reduction potential of TCB is 0.96 V more negative than that of TCT and should only occur upon reaction with CoCp*$_2$ of the reductants available to us. This reaction led to the isolation of a compound of [CoCp*$_2$][TCB] composition, whose structure was determined to be {[CoCp*$_2$]$^+$}$_2$[TCB]$_2^{2-}$, Figure 6b. The [TCB]$_2^{2-}$ dianion results from dimerization at the nonsubstituted ring carbon, which is at variance with the proposed structure of **2**$^{2-}$. [TCB]$_2^{2-}$ has a central C−C bond of 1.560 (5) Å, and the bond lengths within the benzene rings are C50−C51, 1.509(4) Å; C51−C52, 1.362(4) Å; C52−C53, 1.424(4) Å; C53−C54, 1.405(4) Å; C54−C55, 1.364(3) Å; and C55−C50, 1.523(3) Å. There is a shift of the ring

SCHEME 1
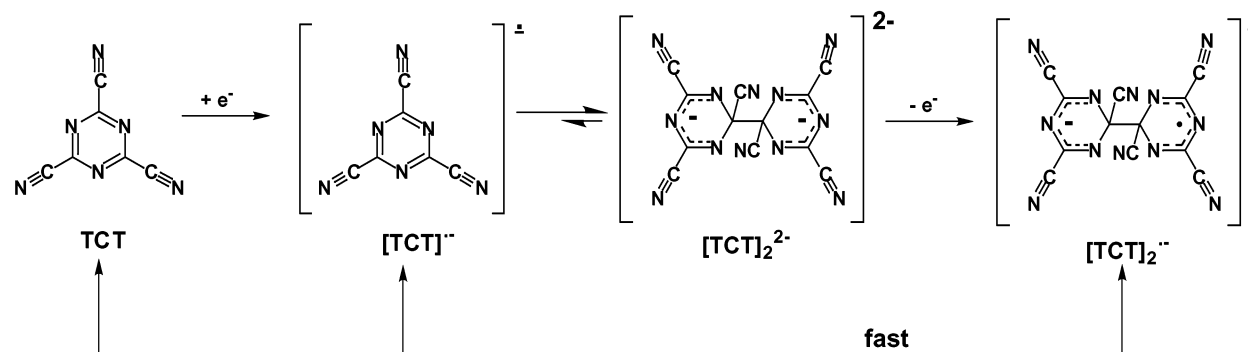
$\nu_{C=C}$ stretch at 1430 cm^{-1} in TCB to 1497 cm^{-1} in [TCB]$_2{}^{2-}$, again indicating that there is a negative charge within the ring, as observed for [TCT]$_2{}^{2-}$. The C–H stretch disappears upon reduction; however, an expected new peak does not appear. The [TCB]$^{•-}$ dimerization at the unsubstituted carbons, as opposed to the nitrile-substituted carbons, is due to the spin density of the radical anion being the greatest at the unsubstituted carbons. This most likely forms a kinetically stabilized product as it precipitates immediately upon the reduction of TCB with CoCp*$_2$.[20] [TCB]$_2{}^{2-}$ can be oxidized to TCB^0 with 2,3-dichloro-5,6-benzoquinione (DDQ), i.e., via cleavage of the central dimer C–C bond, analogous to the TCT oxidation mechanism shown in Scheme 1.

[TCB]$_2{}^{2-}$
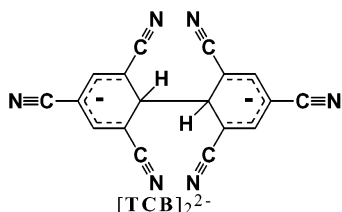
Formation of C$_{10}$N$_{10}$, TCBT. In addition to formation of the charge-transfer complex [TMPD][TCT], the reaction of TCT with the weak reducing agent TMPD led to isolation of a compound of [TMPD][C$_{10}$N$_{10}$] composition in low yield (~2%). The structure of [TMPD]-[C$_{10}$N$_{10}$] was determined by single-crystal X-ray diffraction and reveals that C$_{10}$N$_{10}$ is the new cyanocarbon 4,4′,6,6′-tetracyano-2,2′-bitriazine, TCBT, Figure 7. [TMPD][TCBT] is valence ambiguous, because it can be formulated as either [TMPD]^0[TCBT]^0, [TMPD]$^{•+}$-[TCBT]$^{•-}$, or [TMPD]$^{2+}$[TCBT]$^{2-}$.

As the reduction is irreversible, it is possible that a small fraction of TCT is reduced and dimerized to [TCT]$_2{}^{2-}$ and then forms TCBT through the loss of two cyanides. Hence, only a small amount of TCBT forms, as observed.

The IR spectrum of TCT of [TMPD][TCBT] has ν_{CN} absorptions occurring as a three-band pattern (2269, 2254, and 2241 cm^{-1}) but is shifted slightly higher in energy by ~10 cm^{-1} with respect to TCT. Also present for TCBT are absorptions at 1342, 1250, and 766 cm^{-1},

(20) The theory of the kinetically stabilized product is suggested on the basis of other reported examples: (a) Effenberger, F.; Mack, K. E.; Niess, R.; Reisinger, F.; Steinbach, A.; Stohrer, W.-D.; Stezowski, J. J.; Rommel, I.; Maier, A. *J. Org. Chem.* **1988**, *53*, 4379. (b) Heinze, J.; Willmann, C.; Bäuerle, P. *Angew. Chem., Int. Ed.* **2001**, *40*, 2861.
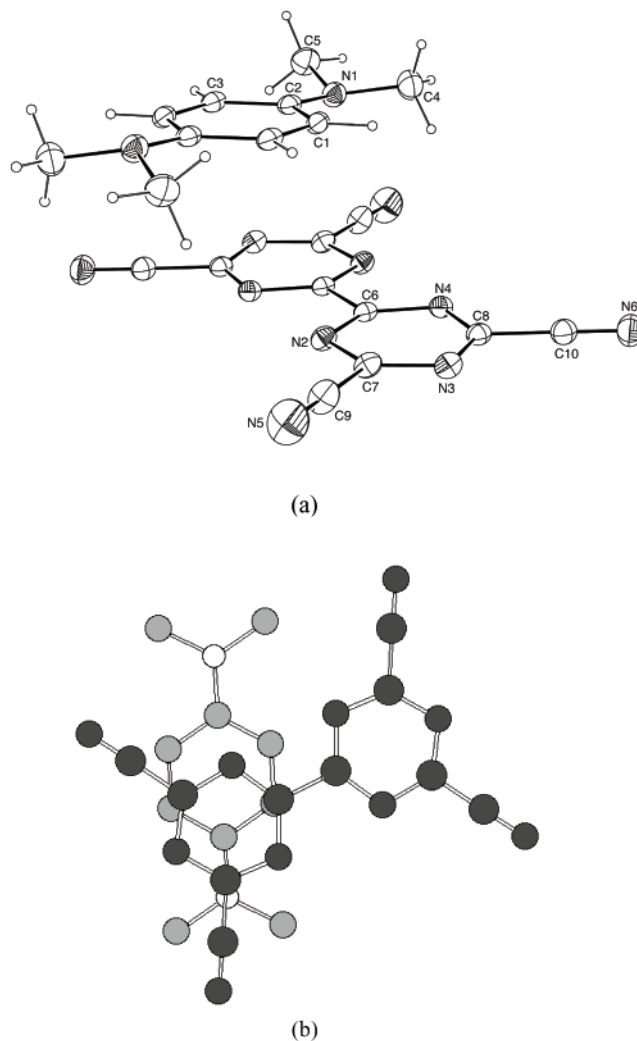
(a)

(b)

FIGURE 7. (a) ORTEP drawing (50%) of [TMPD][TCBT] and (b) view of the offset stacking of TMPD and TCBT rings, where TMPD are the lighter spheres and TCBT the darker spheres. Bond lengths for the triazine rings are 1.3333 (15) Å for C6–N2, 1.3332 (15) Å for N2–C7, 1.3335 (16) Å for C7–N3, 1.3285 (16) Å for N3–C8, 1.3298 (15) Å for C8–N4, and 1.3402 (16) Å for N4–C6. Bond angles around the ring nitrogens are 113.43, 112.41, and 113.10 (10)° for C6–N2–C7, C7–N3–C8, and C8–N4–C6, respectively, while those around the ring carbons are 126.08, 127.21, and 127.73 (10)° for N4–C2–N2, N2–C7–N3, and N3–C8–N4, respectively.

which are not present in the spectrum of [TMPD][TCT]. The resulting complex is diamagnetic and EPR silent,

suggesting but not conclusively showing, as dimerization may occur, that the product is a charge-transfer complex and not a one-electron-transfer salt, [TMPD]•+[TCBT]•−. The electrochemical behavior of [TMPD][TCBT] has a reversible reduction of TCBT (TCBT/[TCBT]•−) at +0.03 V, which is noticeably different from the reduction of TCT, Figure 1d. Also present are the TMPD redox pairs of TMPD$^{0/+}$ and TMPD$^{+/2+}$ at +0.10 and +0.72 V, respectively.[11]

The formulation of [TMPD]^0[TCBT]^0 is principally based on the structure of the TMPD molecule as a function of its charge. The TMPD ring bond lengths are 1.3800 (18) Å for C1−C1′ and 1.4050 (18) Å for C2−C3 within the TMPD ring, and the C2−N1 bond length is 1.3923 (16) Å; these values are in good agreement with the 1.39 Å reported for TMPD^0.[21a] In contrast, for [TMPD]•+ as the [I$_3$]− and [ClO$_4$]− salts, the corresponding bond lengths are 1.362 ± 0.001, 1.426 ± 0.004, and 1.346 ± 0.002 Å.[21b,c] Thus, the interatomic TMPD distances, particularly the C2−N1 distance, are characteristic of TMPD^0, not [TMPD]•+.

The two triazine rings of TCBT in the TMPD charge-transfer complex are connected by a 1.492 (2) Å C−C bond, as expected for a sp^2−sp^2 single C−C bond and observed in the structure of bipyrimidine, which has a central C−C bond of 1.498 Å.[22] All of the bond lengths within the rings are 1.34 ± 0.01 Å, and the bond angles are 127 and 113° for the N−C−N and C−N−C angles, respectively, within the ring, as seen in most neutral triazine ring systems.[4b] The TMPD and TCBT planes stack along chains with alternating TMPD and TCBT moieties and deviate from coplanarity by 1.73°, with each TCBT fragment displaced from the next TCBT in the chain by a half unit. The planes are approximately 3.1 Å apart, with the closest contact to the cyano-substituted ring carbon of the triazine (C8) being the TMPD nitrogen (N1) with a distance of 2.903 Å. The short contact results in a slight deviation of planarity of the dimethylamino group with respect to the TMPD central ring, as the nitrogen is electrostatically attracted toward the triazine ring.

2,2′-Bitriazines are rare, with only four other examples previously reported, **3a−d**, in which the 4- and 6-positions are substituted with electron-donating groups.[23] This is the first structurally characterized bitriazine reported. The azide **3d** (Y = N$_3$) has been postulated as a product in the decomposition of 2,4,6-triazido-1,3,5-triazine en route to nitrogen-rich carbon nitride network solids but has not been isolated.[24] However, TCBT could not be isolated from [TMPD][TCBT] by either sublimation or solvent extraction, as TMPD and TCBT cosublime and have similar solubilities. This bitriazine could be of interest in the development of molecule-based magnets or three-dimensional network structures in general due to the number of possible coordination sites for metals

(21) (a) Ikemoto, I.; Katgiri, G.; Nishimura, S.; Yakushi, K.; Kuroda, H. *Acta Crystallogr., Sect. B* **1979**, *B35*, 2265. (b) de Boer, J. L.; Vos, A.; Huml, K. *Acta Crystallogr.* **1968**, *B24*, 542. (c) de Boer, J. L.; Vos, A. *Acta Crystallogr.* **1972**, *B28*, 835.
(22) Fernholt, L.; Romming, C.; Samdal, S. *Acta Chem. Scand. Ser. A* **1981**, *35*, 707.
(23) Kitajima, H.; Nakatsuji, A.; Yamauchi, H. *Nippon Kagaku Kaishi* **1982**, *8*, 1425.
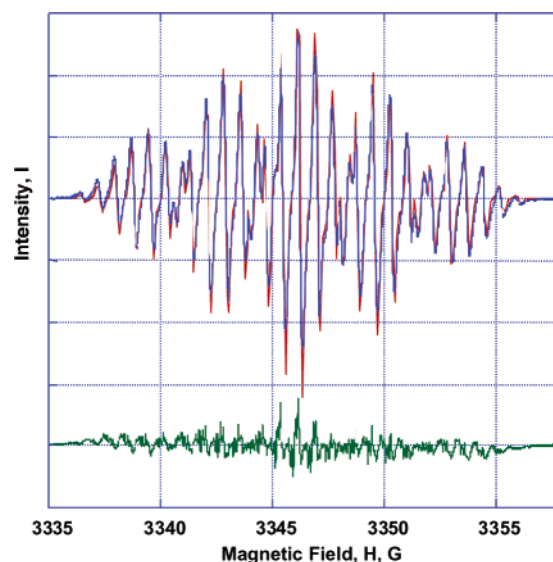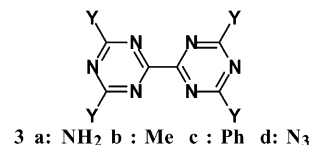(24) Gillian, E. G. *Chem. Mater.* **2000**, *12*, 3906.

FIGURE 8. EPR signal (red) and fit (blue) for [TDAE]$^{2+}$-{[TCBT]•−}$_2$ in THF at room temperature. Fit was made with ^{2}A$_{^{14}N}$ = 3.347 G and ^{4}A$_{^{14}N}$ = 0.764 G. The difference between the calculated and observed spectra is in green at the bottom.

as well as its reversible one-electron reduction to the radical anion.

3 a: NH$_2$ b : Me   c : Ph d: N$_3$

Formation of [C$_{10}$N$_{10}$]•−, [TCBT]•−. Reduction of TCT with either Cr(mes)$_2$, CoCp*$_2$, or TDAE, results in a second deeply colored product in addition to formation of the dimer [TCT]$_2$$^{2−}$. The solid-state EPR spectra of all three reduction products from the reaction with Cr(mes)$_2$, CoCp*$_2$, or TDAE indicate the presence of a radical, A•−, with g = 2.003. Dissolution of any of these products in either MeCN or THF allows the resolution of the EPR hyperfine splitting pattern due to the coupling of the radical with the S = 1 ^{14}N nucleus. The observed spectrum is identical to that reported for the in situ Na or K reduction of TCT, and **1**•− was postulated as the resulting product.[7] Our room-temperature EPR spectrum could be fit with g = 2.0035 and with a set of two equivalent nitrogens with ^{2}A$_{^{14}N}$ = 3.347 G, a value characteristic of aza ring nitrogens,[25] and a set of four equivalent nitrogens with ^{4}A$_{^{14}N}$ = 0.765 G and a line width of 0.240 G, Figure 8. These values are similar to those previously reported with ^{2}A$_{^{14}N}$ = 3.78 G and ^{4}A$_{^{14}N}$ = 0.82 G,[7] as evidenced by the difference spectrum, Figure 8. The 2:4 nitrogen ratio is inconsistent with the structure of [TCT]•−, which led Carrington et al. to propose two possibilities: (1) a molecular rearrangement to **1**•−, which would support a 2:4 ratio, or (2) a Jahn−Teller distortion of the radical anion of TCT. Although reduction of some alkyl triazines with Zn/MeCO$_2$H decompose upon heating (through the loss of NH$_3$) to form trialkylimidazoles, Scheme 2,[26] analogous formation of

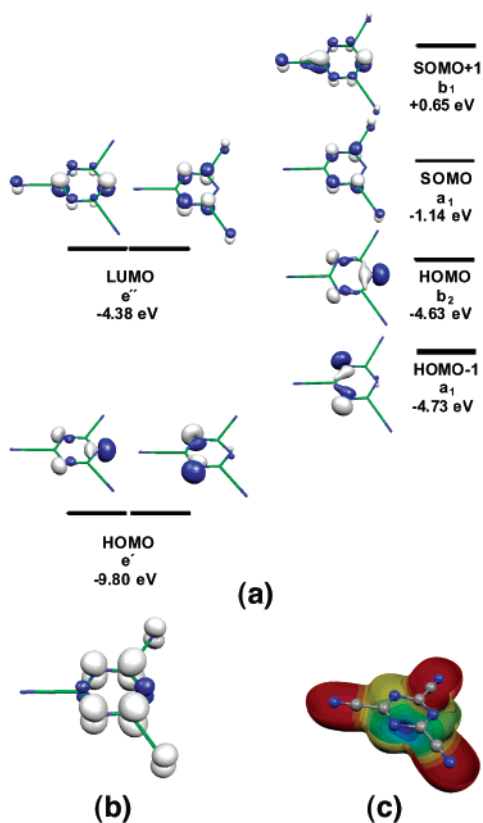(25) The symbol "x" in ^{x}A$_{^{14}N}$ represents the number of equivalent nitrogens.

FIGURE 9. (a) Calculated molecular orbital diagram for TCT⁰ and [TCT]•⁻ species with 90% of the charge plotted at a contour of 0.01 e⁻, (b) the spin density of [TCT]•⁻ showing 95% of the spin at a contour of 0.005 e⁻, showing sets of equivalent nitrogens of 2:2:1:1, and (c) the predicted charge density for [TCT]•⁻ species, where red and blue represent negative (−) and positive (+) potentials, respectively.

SCHEME 2

R = Me, Et, Ph
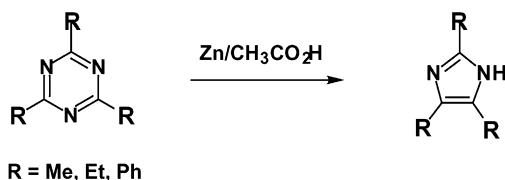
the fused imidazole **1**•⁻ is mechanistically unreasonable due to the number of bonds that need to be broken and formed.

It was also suggested that a distortion of the structure of [TCT]•⁻, due to breaking the degeneracy of two LUMO orbitals of TCT following reduction, could explain the 2:4 nitrogen ratio.[7] Thus, the structure of [TCT]•⁻ was computationally investigated to ascertain if a distortion occurs and, if so, the predicted EPR spectrum. Density functional theory (DFT) calculations at the B3LYP level using 6-31+G(2d,2p) basis sets were carried out on the neutral and radical anion of TCT. The TCT contains a set of degenerate e' HOMO orbitals and a set of degenerate e'' LUMO orbitals, with the structural symmetry being D_{3h}. Upon addition of an electron to form [TCT]•⁻, the degeneracies are broken as the symmetry of the molecule is reduced to C_{2v}. Thus, a Jahn−Teller distortion

(26) Cook, A. H.; Jones, D. G. *J. Chem. Soc.* **1941**, 278.

is predicted upon reduction, and the resulting SOMO and calculated spin density of [TCT]•⁻, Figure 9b, indicate that a 2:2:1:1 ratio of inequivalent nitrogens using the atom labels in Table 1 would result with predicted hyperfine splittings of 3.44 (N1,N3), 1.41 (N2), 2.73 (N5,N6), and 0.18 (N4) G, respectively. Hence, although a distortion is anticipated for [TCT]•⁻, its predicted EPR spectrum is inconsistent with that observed.

Furthermore, the CV of [TDAE]²⁺[A•⁻]₂ does not show the irreversible oxidation and reduction characteristic of TCT, but a new, reversible one-electron peak at +0.03 V (vs SCE) appears, Figure 1e. This peak at +0.03 V is identical to that observed for [TMPD][TCBT]. Likewise, the elemental analysis of the [TDAE]²⁺[A•⁻]₂ also suggests that A•⁻ is [TCBT]•⁻. Therefore, although **1**•⁻ is not expected on the basis of the number of bonds that would have to be broken and reformed, the experimental EPR, as compared with the predicted spectra, the elemental analysis, and the difference in electrochemical behavior of A•⁻, as compared with the behavior of TCT and [TCT]•⁻, suggest that a new species is formed following the reduction of TCT and is [TCBT]•⁻. Formation of [TCBT]•⁻ can be expected via more reasonable mechanistic processes as compared to **1**•⁻ (vide infra).

DFT calculations of TCBT and [TCBT]•⁻ were carried out at the B3LYP level, and the MO diagram as well as the spin and charge densities were calculated, Figure 10 and Table 1. TCBT contains two closely spaced, but not degenerate, HOMO and HOMO-1 orbitals. Upon addition of an electron to form the radical anion, [TCBT]•⁻, all of the orbitals increase in energy, with the two highest filled still lying fairly close in energy to one another. The LUMO orbital and spin density of [TCBT]•⁻ are predicted to be localized predominantly within the rings, with a minimal spin residing on the nitrile nitrogen atoms, Table 1 and Figure 10b. The resulting D_{2h} symmetry of the spin density would propose a set of 2 and a set of 4 equivalent nitrogens within the rings and another set of 4 equivalent nitrogens due to the nitriles. While strong coupling of the spin to the two sets of nitrogens within the rings are expected, weaker coupling to the nitriles is also expected, as there is very little spin density on the nitriles (<0.003 e⁻). This is consistent with the observed EPR splittings, with a set of 2 and a set of 4 equivalent nitrogens with strong coupling to the ring nitrogens. The broad peaks (0.24 G line width) in the spectra obtained could be due to the concomitant weak splitting of the peaks from the nitrile groups, but the sensitivity of the instrument does not allow this very weak coupling (<0.1 G) to be resolved. In contrast to the spin density, the charge resides on the nitrile and imide Ns, Figure 10c and Table 1.

All three compounds possessing [TCBT]•⁻ have the same IR with absorptions at 1530, 1275, 1180, 950, 915, and 775 cm⁻¹, as well as a weak $v_{C≡N}$ absorption at 2242 cm⁻¹. Furthermore, the solution (MeCN) UV/visible spectra of the three [TCBT]•⁻-containing compounds have several identical absorptions centered at ∼18 000 cm⁻¹ (556 nm), Figure 11, in addition to those attributed to the cation. This lower-energy absorption is assigned to the $b_{2g}^2 b_{3u}^1 → b_{2g}^1 b_{3u}^2$ (HOMO−SOMO) transition of the radical anion, as seen in the MO diagram for [TCBT]•⁻, Figure 10a. This absorption is split into five distinguishable peaks separated by approximately 1430 cm⁻¹, which
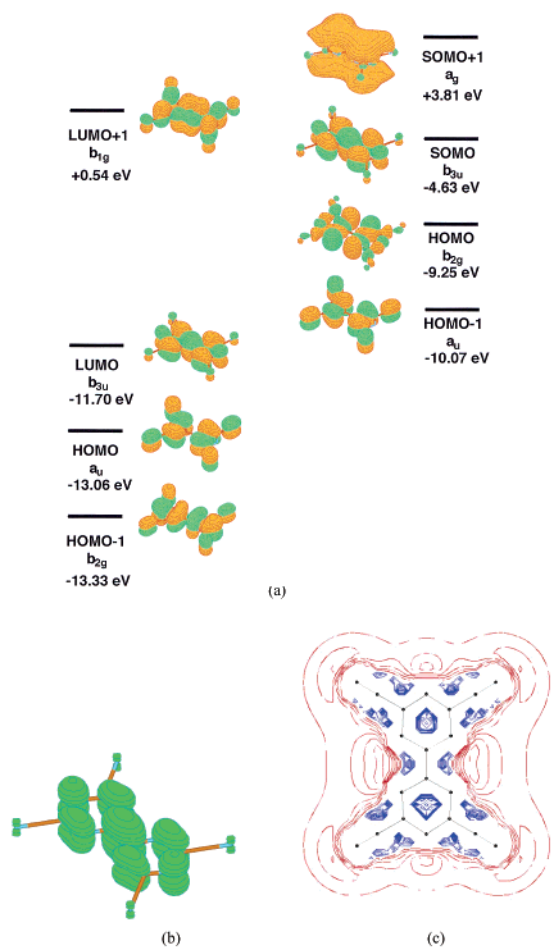
FIGURE 10. (a) Calculated molecular orbital diagram for TCBT⁰ and [TCBT]•⁻ species with 90% of the charge plotted at a contour of 0.017 e⁻, (b) the spin density of [TCBT]•⁻ showing 90% of the spin at a contour of 0.002 e⁻, showing sets of equivalent nitrogens of 2:4:4, and (c) the predicted charge density for [TCBT]•⁻ species, where red and blue represent negative (−) and positive (+) potentials, respectively.

are attributed to vibrational overtones due to phonon coupling with the excited state of the radical anion, similar to that noted for [TCNE]•⁻.[27]

The $\sim$1430 cm⁻¹ splittings observed within the 18 000 cm⁻¹ (556 nm) absorption correspond very closely to the energy of the ground-state $\nu_{C \equiv N}$ absorption of 1530 cm⁻¹. The $\sim$100 cm⁻¹ decrease in frequency is due a decrease in the ring CN bond lengths in the excited state, as the p* orbital is a bonding orbital for some C=N bonds and antibonding for the other C=N bonds within the ring, and the population of the p* would both increase and decrease C=N bonds, resulting in a symmetric (D_{2h}) distortion of the [TCBT]•⁻, with little change in the nitrile bonds, as seen in the change bond lengths calculated in Table 2.

The radical anion has a higher-energy absorption at 29 000 cm⁻¹ (345 nm), which is attributed to the $b_{3u}^1 b_{1g}^0 \rightarrow b_{3u}^0 b_{1g}^1$ transition, which is consistent with the calculations, Figure 10a. The $b_{3u}^1 b_{ag}^0 \rightarrow b_{3u}^0 a_g^1$ transition is

(27) (a) Dixon, D. A.; Miller, J. S. *J. Am. Chem. Soc.* **1987**, *109*, 3656. (b) Miller, J. S.; Krusic, P. J.; Dixon, D. A.; Reiff, W. M.; Zhang, J. H.; Anderson, E. C.; Epstein, E. J. *J. Am. Chem. Soc.* **1986**, *108*, 4459. (c) Haller, I.; Kaufman, F. B. *J. Am. Chem. Soc.* **1976**, *98*, 1464.
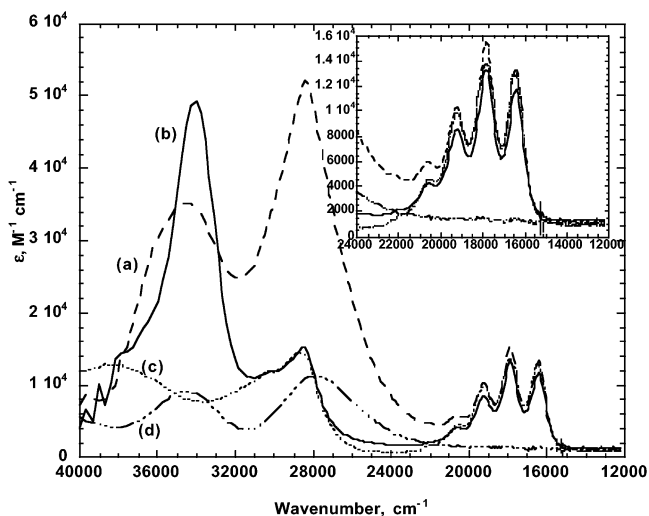
FIGURE 11. Molar extinctions of (a) [Cr(mes)₂]⁺[TCBT]•⁻ (dashed line), (b) [CoCp*₂]⁺[TCBT]•⁻ (solid line), (c) [TDAE]²⁺-{[TCBT]•⁻}₂ (dotted line), and (d) {[Cr(mes)₂]⁺}₂[TCT]₂²⁻ (dashed solid line) as solutions in MeCN. Inset shows the vibrational coupling of [TCBT]•⁻.

TABLE 2. Optimized Geometries of Neutral and Radical Anion of [TCBT]ⁿ (*n* = 0, 1−) from Calculations at the Density Functional B3LYP/6-31++G(2d,2p) Level[a]

[TCBT]ⁿ

bond	bond length (Å) $n = 0$	bond length (Å) $n = 1-$	% change
a	1.506	1.406	−6.6%
b	1.315	1.363	+3.7%
c	1.314	1.295	−1.4%
d	1.316	1.335	+1.4%
e	1.455	1.462	+0.5%
f	1.133	1.136	+0.3%

[a] Resulting geometries for both species have D_{2h} symmetry.

inappropriate for use in making this assignment, because the anion's a_g SOMO + 1 orbital is a virtual diffuse Rydberg orbital that is more appropriate to the dianion than to the anion.

The magnetic susceptibility, χ, of the salts of the [TCBT]•⁻ was determined between 2 and 300 K. The room-temperature-effective magnetic moments, μ_{eff} [= $(8\chi T)^{1/2}$] are 1.72, 2.34, and 2.43 μ_B for [CoCp*₂]-[TCBT]•⁻, [Cr(mes)₂]⁺[TCBT]•⁻, and [TDAE]²⁺[[TCBT]•⁻]₂, respectively. The values are consistent with one spin for the former compound and two spins for the latter two compounds as expected. The 2.34 μ_B moment is reduced from the expected 2.45 μ_B due to the presence of an impurity, most likely diamagnetic [TCT]₂²⁻. The $\chi(T)$ can be modeled as typical Curie−Weiss behavior, $\chi \propto [T - \theta]^{-1}$, and [TDAE]²⁺{[TCBT]•⁻}₂ and [Cr(mes)₂]⁺[TCBT]•⁻ show weak antiferromagnetic coupling, with $\theta = -3.6$ and −0.2 K, respectively. In contrast, [CoCp*₂][TCBT]••⁻ exhibits weak ferromagnetic coupling, with $\theta = +3.8$ K.

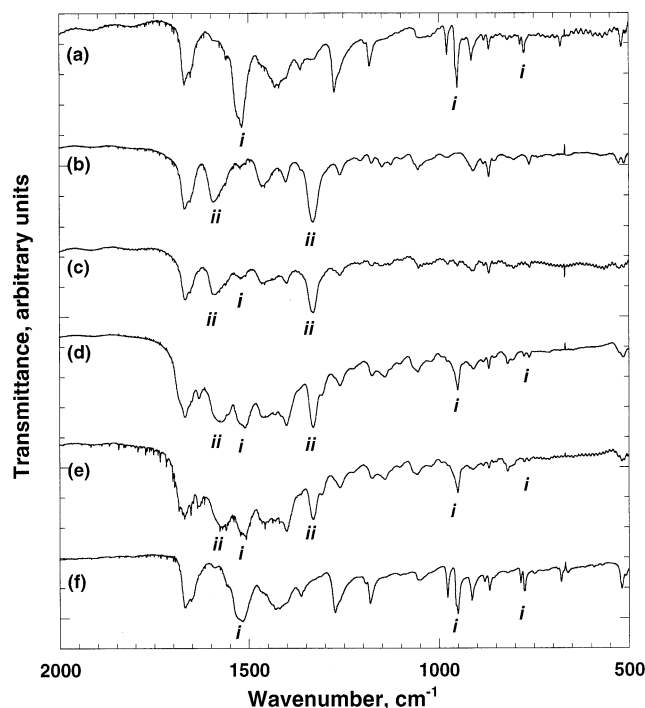**FIGURE 12.** IR spectra of (a) [TDAE]$^{2+}${[TCBT]$^{\cdot-}$}$_2$, (b) [TDAE]$^{2+}$[TCT]$_2^2$, and [TDAE]$^{2+}$[TCT]$_2^{2-}$ thermolyzed for (c) 1, (d) 12, and (e) 24 h and (f) recrystallized after 24 h, as KBr pellets. Peaks labeled *i* are characteristic peaks for [TCBT]$^{\cdot-}$, and those labeled *ii* are characteristic for [TCT]$_2^{2-}$.

The IR spectrum of [TDAE]$^{2+}${[TCBT]$^{\cdot-}$}$_2$ is identical to the thermolysis product isolated from TGA/MS experiments of the [TDAE]$^{2+}$[TCT]$_2^{2-}$, in which the sample was heated until the loss of [CN$^{\cdot}$] was detected in the mass spectrometer. Solid [TDAE]$^{2+}$[TCT]$_2^{2-}$ was heated to 110 °C, simulating the conditions of the TGA experiment to effect the mass loss of [CN]$_x$. A portion of the sample was removed after 1, 12, and 24 h of heating, and its IR spectra were obtained, Figure 12. The solid that remained after 24 h was recrystallized from MeCN. As [TDAE]$^{2+}$-[TCT]$_2^{2-}$ is heated and decomposes, the intensity of the characteristic absorptions for [TCT]$_2^{2-}$ decrease (peaks labeled as *ii*) while characteristic peaks for the [TDAE]$^{2+}$-{[TCBT]$^{\cdot-}$}$_2$ sample increases (peaks labeled as *i*). This suggests that following formation [TCT]$_2^{2-}$, loss of CN$^{\cdot}$ and CN$^-$ occurs, which results in the formation of [TCBT]$^{\cdot-}$, most likely through the intermediate [C$_{11}$N$_{11}$]$^{\cdot 2-}$, Scheme 3. The final product of thermolysis would therefore be the two salts [TDAE]$^{2+}${[TCBT]$^{\cdot-}$}$_2$ and [TDAE]$^{2+}$-[CN$^-$]$_2$. [TCBT]$^{\cdot-}$ is responsible for the 2N:4N EPR signal that is observed in both the direct reduction of TCT with TDAE, Na, or K and in the recrystallized thermolysis product of [TCT]$_2^{2-}$. As the decomposition product of [TCT]$_2^{2-}$ involves the loss of mass, it is likely that [TCT]$^{\cdot-}$ is neither present nor the species responsible for the observed EPR spectra.

Time-resolved, stopped-flow IR studies were performed on the reaction mixture, with the first spectra beginning at 50 ms following mixing, and recorded approximately every 15 s over the course of 11 min, Figure 13a. The first scan shows the presence of a large peak at 1670 cm^{-1}, characteristic of the [TDAE]$^{2+}$,[28] indicating that the electron transfer from TDAE to TCT occurs in less than

20 ms, the detection limit of the system. Additionally, peaks characteristic of both [TCT]$_2^{2-}$ and [TCBT]$^{\cdot-}$ are also present immediately, suggesting that dimerization and the initiation of decomposition to [TCBT]$^{\cdot-}$ also require <20 ms. This suggests that the intermediate in the transformation has characteristics of both [TCT]$_2^{2-}$ and [TCBT]$^{\cdot-}$, which could possibly be [C$_{11}$N$_{11}$]$^{\cdot 2-}$. This is also consistent with the electrochemical behavior of TCT being irreversible at even the greatest scan rates studied (2000 mV/s). Monitoring of the peaks characteristic of [TCT]$_2^{2-}$, at 1590 and 1330 cm^{-1}, as a function of time shows the gradual decrease in intensity, along with the simultaneous increase of intensity of the characteristic peaks of [TCBT]$^{\cdot-}$ at 1530 and 950 cm^{-1}, Figure 13b. Hence, the decomposition of [TCT]$_2^{2-}$ to [TCBT]$^{\cdot-}$ occurs in a multistep process, as seen in the change in slopes in Figure 13b during the experiment. However, the kinetics is not well understood and still under investigation. Nonetheless, it is apparent that the reduction of TCT results in a very rapid dimerization followed by a slower decomposition to form the new radical anion [TCBT]$^{\cdot-}$.

[Cr(mes)$_2$]$^+$[TCBT]$^{\cdot-}$ and [CoCp*$_2$]$^+$[TCBT]$^{\cdot-}$ display the same EPR splittings, as well as an IR similar pattern to that of [TDAE]$^{2+}${[TCBT]$^{\cdot-}$}$_2$. However, pure samples of [Cr(mes)$_2$]$^+$[TCBT]$^{\cdot-}$ could not be obtained, as it cocrystallizes from solution with the respective salt of [TCT]$_2^{2-}$. Thermolysis experiments, similar to that of the [TDAE]$^{2+}$ salt decomposes [TCT]$_2^{2-}$ forming salts of [TCBT]$^{\cdot-}$, could not be carried out on the [Cr(mes)$_2$]$^+$-[TCBT]$^{\cdot-}$ and [CoCp*$_2$]$^+$[TCBT]$^{\cdot-}$ due to the decomposition of the cations upon heating to temperatures sufficient to effect the loss of [CN]$_x$ from [TCT]$_2^{2-}$.

Mechanistic Considerations. Several feasible mechanisms for the formation of TCBT and [TCBT]$^{\cdot-}$ from the reduction of TCT are shown in Scheme 3. The most feasible of these is Scheme 3a, which goes through the dimer dianion intermediate [TCT]$_2^{2-}$, which has been isolated from the direct reduction of TCT and, as discussed, decomposes to form [TCBT]$^{\cdot-}$ on the basis of thermolysis and spectroscopic data. When heated or allowed to stand for extended periods of time (1 day or longer), [TCT]$_2^{2-}$ can lose CN$^{\cdot}$, which evolves as C$_2$N$_2$, both of which are seen in the mass spectra (MS) during the TGA/MS experiments as they are evolved from the solid salts of [TCT]$_2^{2-}$. This results in the formation of [C$_{11}$N$_{11}$]$^{\cdot 2-}$, which could lose CN$^-$ in solution to yield [TCBT]$^{\cdot-}$. In the thermolysis of solid [TDAE]$^{2+}$[TCT]$_2^{2-}$, the presence of [TCT]$_2^{2-}$ is evident in the IR of the sample until the thermolysis product is *recrystallized*, suggesting that the dissolution is required to lose a charged species such as CN$^-$, ultimately yielding [TCBT]$^{\cdot-}$. The solution-phase, time-resolved IR spectra also indicate the presence of both [TCT]$_2^{2-}$ and [TCBT]$^{\cdot-}$ after the initial reduction, Figure 13, and the ensuing simultaneous decomposition of [TCT]$_2^{2-}$ and formation of [TCBT]$^{\cdot-}$ also support this mechanism.

Scheme 3, which goes through intermediate [TCT]$_2^{\cdot-}$, is also feasible. As TMPD is a weak donor and only reduces ~0.01% of TCT, it is extremely unlikely for two [TCT]$^{\cdot-}$ to react together in the reaction mixture to eventually yield TCBT. In contrast, [TCT]$^{\cdot-}$ may react

(28) Pokhodnia, K. I.; Papavassilou, J.; Umek, P.; Omerzu, A.; Mihailovic, D. *J. Chem. Phys.* **1999**, *110*, 3606.
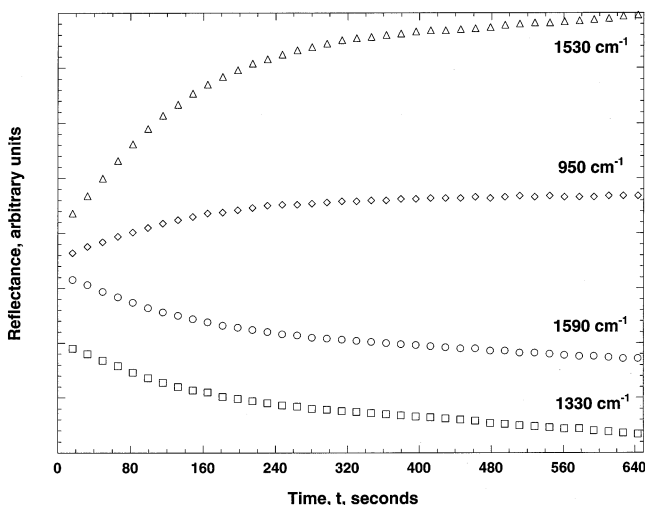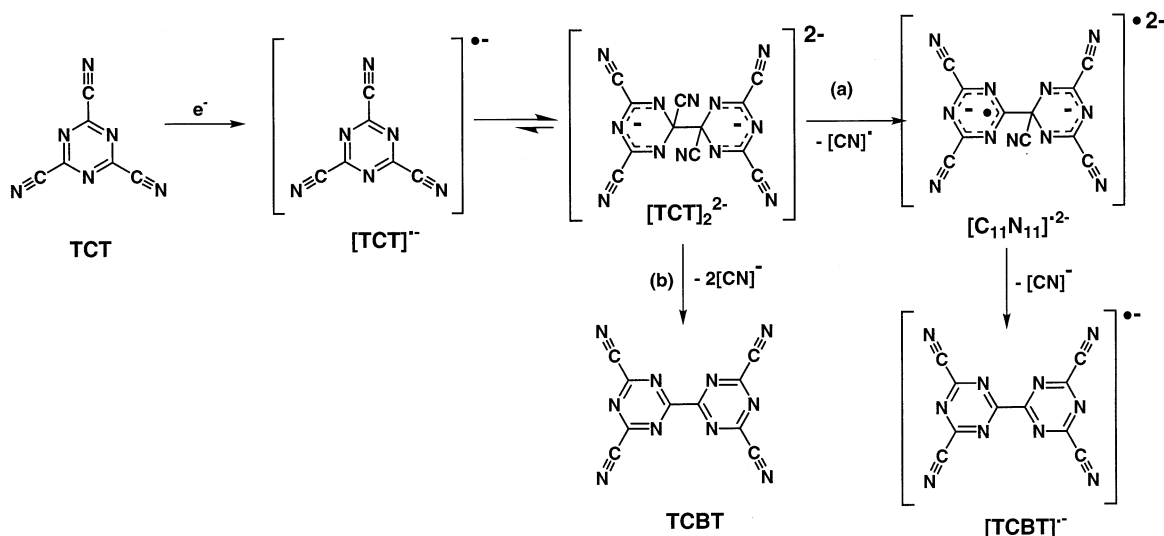
SCHEME 3

FIGURE 13. Time dependence of IR absorptions at 1530, 950, 1590, and 1330 cm^{-1} for the reaction of TDAE and TCT in MeCN using a stopped-flow reaction mixer. Peaks at 1530 and 950 cm^{-1} are characteristic of [TCBT]$^{•-}$, and the peaks at 1590 and 1330 cm^{-1} are characteristic of [TCT]$_2{}^{2-}$.

with neutral TCT to form [TCT]$_2{}^{•-}$. However, the electrochemical behavior of [TCT]$_2{}^{•-}$ shows that it is unstable, as evidenced by the irreversible oxidation of [TCT]$_2{}^{2-}$ in the different salts produced, e.g., Figure 1d. This irreversibility could be due to [TCT]$_2{}^{•-}$ decomposing to form either [TCBT]$^{•-}$ or [TCT]$^{•-}$ and TCT^0, Scheme 1.

The loss of two CN$^-$ fragments simultaneously from the intermediate [TCT]$_2{}^{2-}$ and formation TCBT, Scheme 3b, are possible. This, however, is unlikely, as CN$^-$ should not simply be eliminated from the salts in the solid state as seen in the thermolysis experiments. Also, if two [CN]$^-$ fragments are lost, the result would be a [cation]$^+$[CN]$^-$ salt and TCBT^0 in solution. The original reducing agents would then exist as cations in ion pairs with the cyanide anions, and there would be little, if any, reducing agent left to reduce the resulting neutral TCBT to its radical anion. As the yields of the electron-transfer reactions with TDAE, Co^{II}Cp*$_2$, and Cr^0(mes)$_2$ are significant ($\geq$20%), this mechanism is not probable.

Conclusion

The radical anion of TCT, [TCT]$^{•-}$, is unstable in solution as seen in the electrochemical experiments, as well as by the isolation of [TCT]$_2{}^{2-}$. Reaction of TCT with strong electron donors results in an electron-transfer producing the unstable [TCT]$^{•-}$, which then dimerizes as salts of [TCT]$_2{}^{2-}$. Instability of tricyanoarenes is also seen in the reduction of TCB to form [TCB]$_2{}^{2-}$, which dimerizes at the unsubstituted carbon of the benzene ring, as opposed to the nitrile-substituted carbon as previously predicted and as observed for [TCT]$_2{}^{2-}$.

Reaction of TCT with weak electron donors such as TMPD and TTF results in charge-transfer complexes of TCT, which in the presence of trace water, undergoes nucleophilic substitution to form DCTOH, which in the presence of a sufficiently strong base such as TMPD undergoes an acid–base reaction forming [DCTO]$^-$. Decomposition of [TCT]$_2{}^{2-}$ in the solid state or solution ultimately produces the radical anion of [TCBT]$^{•-}$; the neutral species of which was isolated and structurally characterized from the reaction of TCT with TMPD. Mechanistic analysis suggests that the irreversible reduction of TCT occurs via dimerization of [TCT]$^{•-}$ to [TCT]$_2{}^{2-}$, which then decomposes to [TCBT]$^{•-}$ and, hence, is responsible for the previously mysterious 2:4 nitrogen ratio observed in the EPR spectrum. The low charge and spin densities on the terminal nitriles suggest that TCBT and [TCBT]$^{•-}$ will be poor ligands as well as poor spin-coupling linkages, and their use is unlikely to lead to new molecule-based magnets. However, if metal coordination of the ring nitrogens in [TCBT]$^{•-}$ occurs, as observed for bipyridine- and bipyrimidine-containing structures, analogous building of network structures may occur with the possibility of magnetic exchange through the spin-bearing [TCBT]$^{•-}$ ligand.

Experimental Section

All reactions were carried out in a drybox under nitrogen. All solvents were dried by distillation under nitrogen over CaH$_2$ or Na/benzophenone, and all reagents were used as commercially available materials.

Samples for IR spectra were prepared as KBr pressed pellets. Time-resolved infrared spectra were obtained with a

rapid-mixing stopped-flow attachment constructed in-house. The device is centered around on integrated mixer-flow cell based on a microCIRCLE ATR accessory and employed a ZnSe ATR crystal. The effective path length in this configuration is 13 μm. Spectra were collected with a Bruker IFS 66/s spectrometer in rapid-scan mode with a resolution of 8 cm^{-1}.[29] Solid-state UV/visible spectra were performed on KBr pellets of the respective samples (~2% w/w sample/KBr).

Cyclic voltammograms were performed scanning from +1.5 to −2.0 V with scan rates of 2−5000 mV/s, with the reported CVs at 100 mV/s. Pt working and counter electrodes were used with a Ag/AgCl reference electrode charged with [Me$_4$N]Cl, and [NMe$_4$]Cl was used as a supporting electrolyte in acetonitrile (0.10 M). All CVs were referenced to a ferrocene/ferrocenium standard and reported vs SCE.

Thermal properties and mass spectrometry were performed with a thermogravimetric analyzer (TGA), with the gas outlet connected to a mass spectrometer with an ionization potential of 70 eV. Elemental analysis was performed by Complete Analysis Laboaotries, Inc. (Parsippany, NJ).

Magnetic susceptibility measurements were performed between 2 and 300 K at a field of 1000 Oe on a SQUID magnetometer as previously described.[30] EPR spectra were recorded using an X-band spectrometer with 1,1-diphenyl-2-picrylhydrazyl (DPPH) as an external standard ($g = 2.0036$).[31]

Computational studies were performed at the DFT B3LYP level using 6-31+G(2d,2p) basis sets and using RHF theory for the [DCTO]$^-$ and neutral molecules and UHF for the radical anions. Visualization of the molecular orbitals and spin densities were created with MOLDEN for the TCBT species and an in-house version of MOLEKEL for the TCBT species.

X-ray diffraction studies were performed on a CCD diffractometer equipped with Mo Kα ($\lambda = 0.71073$ Å) radiation. All structures were solved by direct methods using the program SIR-97 and refined by the full-matrix least-squares method on F^2 with SHELXL 97.[32a] Anisotropic thermal parameters were assigned to all atoms, except that the hydrogen atoms and their positions were assigned using the riding model. ORTEP diagrams were generated using ORTEP 3.[32b]

1,3,5-Tricyanobenzene, TCB,[33] was prepared using literature methods.

2,4,6-Tricyano-1,3,5-triazine, TCT. The synthesis of TCT is based upon a patent.[34] Solid KCN (15 g, 0.31 mol) was added to a suspension of cyanuric chloride (2,4,6-trichloro-1,3,5-triazine; 17 g, 0.07 mol) in 250 mL of dry MeCN while stirring vigorously at room temperature. The mixture was allowed to stir for 40 h, over which time the mixture turned a brick-red color. The resulting KCl and unreacted KCN were filtered and destroyed in a bleach bath. The solvent of the brown filtrate was removed under reduced pressure, and the oily residue was stirred with 100 mL of CH$_2$Cl$_2$ for 12 h to extract the crude TCT. The insoluble material was filtered out and washed twice more with 100 mL of CH$_2$Cl$_2$. The solvent of the combined filtrates was again removed under reduced pressure, yielding a light brown powder of crude TCT, which was purified by sublimation at 110 °C at ~5 mTorr of pressure with an acetone/CO$_2$ condenser to give white prismatic crystals. Yield: 5.7 g (52%). Mp: 119−121 °C. IR, ν, cm^{-1}: 2301 w, 2277 m, 2252 s, 2063 vw, 1652 m, 1550 m, 1510 s, 1336 s, 938 s,

822 s, 520 s, 422 s. MS, *m/z* (rel %): 52 (39.8), 78 (5.7), 104 (100.0), 156 (M$^+$; 58.6).

[TTF][TCT]. A solution of TTF (200 mg, 0.98 mmol) in 10 mL of MeCN was added to a solution of TCT (152 mg, 0.98 mmol) in 5 mL of MeCN. The solution turned an immediate deep-green color and was allowed to stir for 12 h. The solvent was evaporated and the residue recrystallized from hot MeCN, yielding a blue-green powder. IR, ν, cm^{-1}: 3100 w, 3068 w, 2262 w, 2241 m, 1504 s, 1482 s, 1328 m, 1320 m, 1249 w, 1082 w, 971 w, 936 m, 796 s, 782 m, 733 w, 673 m, 659 m, 516 m. Anal. Calcd for C$_{12}$H$_4$N$_6$S$_4$: C, 39.98; H, 1.12; N, 23.31. Found: C, 40.15; H, 1.29; N, 22.30. Crystal data for [TTF]-[TCT]: C$_{12}$H$_4$N$_6$S$_4$, $M = 360.45$, orthorhombic, space group *Pbca*, $a = 7.1430(1)$ Å, $b = 16.5138(5)$ Å, $c = 25.4640(7)$ Å, $V = 3003.68(13)$ Å^3, $Z = 8$, $\rho_{calcd} = 1.594$ Mg/m^3, absorption coefficient = 0.636 mm^{-1}, $F(000) = 1456$, reflections collected 6305, independent reflections = 3416 [R(int) = 0.0378], GOF = 1.038, $R = 0.0609$, w$R_2 = 0.0951$. CCDC-172417.

[TMPD][TCT]. A solution of TMPD (100 mg, 0.61 mmol) in 5 mL of MeCN was added to a solution of TCT (95 mg, 0.61 mmol) in 5 mL of MeCN. A blue powder immediately precipitated, which was recrystallized from hot MeCN. IR, ν, cm^{-1}: 2957 m, 2891 m, 2851 m, 2806 m, 2256 m, 2246 m, 2235 m, 1610 m, 1521 s, 1497 s, 1479 s, 1330 m, 1317 m, 1213 m, 1178 w, 1130 w, 1056 w, 970 w, 946 m, 829 m, 807 w, 796 s, 660 m, 542 w. Anal. Calcd for C$_{16}$H$_{16}$N$_8$: C, 59.99; H, 5.03; N, 34.98. Found: C, 59.97; H, 5.08; N, 34.90.

[HTMPD]$^+$[DCTO]$^-$. The above procedure was followed exactly, with 0.5 mL of H$_2$O added to the TCT solution before addition of the TMPD, resulting in an immediate yellow precipitate. IR, ν, cm^{-1}: 2960 w, 2904 w, 2860 w, 2819 w, 2249 w, 2224 w, 1580 s, 1540 s, 1523 s, 1446 s, 1361 m, 1309 s, 1235 w, 1186 s, 1055 m, 997 w, 934 m, 910 w, 815 s, 668 w, 547 m. Anal. Calcd for C$_{15}$H$_{17}$N$_7$O: C, 57.87; H, 5.50; N, 31.49. Found: C, 57.87; H, 5.44; N, 31.56. Crystal data for [HTMPD]$^+$-[DCTO]$^-$: C$_{15}$H$_{17}$N$_7$O, $M = 311.36$, monoclinic, space group $P2_1/m$, $a = 10.641(3)$ Å, $b = 6.614(3)$ Å, $c = 11.793(5)$ Å, $\beta = 90.07(3)°$, $V = 830.0(2)$ Å^3, $Z = 2$, $\rho_{calcd} = 1.246$ Mg/m^3, absorption coefficient = 0.085 mm^{-1}, $F(000) = 328$, reflections collected = 6184, independent reflections = 2210 [R(int) = 0.0660], GOF = 0.873, $R = 0.0431$, w$R_2 = 0.1054$. CCDC-172418.

Reduction of TCT with Cr(mes)$_2$ in MeCN. A solution of bis(mesitylene)chromium(0) (100 mg, 0.34 mmol) in 15 mL of MeCN was added to TCT (53 mg, 0.34 mmol) in 5 mL of MeCN. A purple insoluble material formed and was filtered out and identified as [Cr(mes)$_2$]$^+$[TCBT]$^{•-}$ (yield = 44 mg (28%)) by comparison of the IR, UV−vis, and EPR spectra with those of [CoCp*$_2$]$^+$[TCBT]$^{•-}$ and [TDAE]$^{2+}${[TCBT]$^{•-}$}$_2$. IR, ν, cm^{-1}: ([TCBT]$^{•-}$) 2242 vw, 1532 vs, 1274 s, 1179 m, 951 vs, 908 m, 773 m; ([Cr(mes)$_2$]$^+$) 1446 s, 1377 md, 1032 m, 977 m, 440 m. EPR: $g_{\text{TCBT}^{•-}} = 2.0034$, $^2A_{14N} = 3.346$ G, $^4A_{14N} = 0.767$ G (THF, MeCN); $g_{Cr}^I = 1.9872$.

The solvent of the filtrate was allowed to slowly evaporate, resulting in large orange crystals, and determined to be {[Cr(mes)$_2$]$^+$}$_2$[TCT]$_2$$^{2-}$ by single-crystal X-ray diffraction. Yield: 94 mg (61%). IR, ν, cm^{-1}: ([TCT]$_2$$^{2-}$) 2237 vw, 1590 s, 1326 vs, 910 w; (Cr(mes)$_2$$^+$) 1452 m, 1387 m, 1033 m, 1001 w. EPR: $g_{Cr}^I = 1.9873$. Crystal data for {[Cr(mes)$_2$]$^+$}$_2$[TCT]$_2$$^{2-}$· 2MeCN: CCDC-163649.

Reduction of TCT with CoCp*$_2$ and TDAE in MeCN. A solution of the reducing agent (0.30 mmol) in 10 mL of MeCN was added to TCT (47 mg, 0.30 mmol) in 5 mL of MeCN resulting in a purple solution. The solvent was allowed to slowly evaporate to half the original volume and then cooled to 0 °C, allowing a purple precipitate to form that was subsequently filtered and collected. Crystals suitable for single-crystal X-ray diffraction studies could not be isolated.

[CoCp*$_2$]$^+$[TCBT]$^{•-}$. Yield: 6 mg (4%). IR, ν, cm^{-1}: ([TCBT]$^{•-}$) 2243 vw, 1530 vs, 1275 s, 1179 m, 951 vs, 910 m, 775 m; ([CoCp*$_2$]$^+$) 1460 m, 1375 s, 1017 s. EPR: $g_{\text{TCBT}^{•}} = 2.0032$, $^2A_{14N} = 3.347$ G, $^4A_{14N} = 0.764$ G (THF, MeCN). Anal.

(29) Dunn, B. C.; Marda, J. R.; Eyring, E. M. *Appl. Spectrosc.* **2002**, *55*, 751.

(30) Brandon, E. J.; Rittenberg, D. K.; Arif, A. M.; Miller, J. S. *Inorg. Chem.* **1998**, *37*, 3376.

(31) Al'tschuler, S. A.; Kozyrev, B. M. In *Electron Paramagnetic Resonance*; Poole, C. P., Jr., Ed.; Academic Press: New York, 1964; p 298.

(32) (a) Sheldrick, G. M. *SHELX97-2: Program for Crystal Structure Analysis (Release 97-2)*; Universität of Göttingen: Göttingen, Germany, 1998. (b) Farrugia, L. J. *J. Appl. Crystallogr.* **1997**, *30*, 565.

(33) Hill, M.; Mahon, M. F.; Molloy, K. C. *J. Chem. Soc., Dalton Trans.* **1996**, 1857.

(34) Beck, G.; U.S. Patent 5,086,172, 1992.

Calcd for $C_{30}H_{30}N_{10}Co$: C, 61.12; H, 5.13; N, 23.76. Found: C, 60.96; H, 5.01; N, 23.79. Crystals suitable for single-crystal X-ray diffraction studies could not be isolated.

[TDAE]²⁺{[TCBT]·⁻]₂. Yield: 670 mg (37%). IR, ν, cm⁻¹: ([TCBT]·⁻) 2242 vw, 1528 vs, 1275 s, 1179 m, 950 vs, 908 m, 772 m; ([TDAE]²⁺) 1670 s, 1659 s, 1420 s, 1042 w, 865 w, 680 w.²⁶ EPR: $g_{[TCBT]}$· = 2.0039, ²A_{14N} = 3.347 G, ⁴A_{14N} = 0.765 G (THF, MeCN). Anal. Calcd for $C_{30}H_{24}N_{24}$: C, 50.01; H, 3.33; N, 46.70. Found: C, 49.89; H, 3.55; N, 46.58.

Reduction of the volume of the filtrate followed by layering of the filtrate with hexanes resulted in a beige-colored precipitate, determined to be salts of [TCT]₂²⁻.

{[CoCp*₂]⁺}₂[TCT]₂²⁻. Yield: 10 mg (7%). IR, ν, cm⁻¹: ([TCT]₂²⁻) 2237 vw, 1587 s, 1326 vs, 914 w; ([CoCp*₂]⁺) 1471 m, 1382 m, 1024 m. Anal. Calcd for $Co_2C_{52}H_{60}N_{12}$: C, 64.30; H, 6.23; N, 17.32. Found: C, 64.14; H, 6.28; N, 17.04.

[TDAE]²⁺[TCT]₂²⁻. Yield: 210 mg (21%). IR, ν, cm⁻¹: ([TCT]₂²⁻) 2237 vw, 1592 s, 1328 vs, 906 w; ([TDAE]²⁺) 1668 s, 1655 s, 1402 m, 1047 w, 863 w. Anal. Calcd for $C_{22}H_{24}N_{16}$: C, 51.55; H, 4.72; N, 43.73. Found: C, 51.38; H, 4.67; N, 43.84.

[TMPD][TCBT]. Similar reaction conditions were used for the reduction of TCT with CoCp*₂ and TDAE in MeCN in a 1:1 stoichiometric ratio. The resulting solution was left for 2 weeks and the solvent allowed to slowly evaporate, resulting in deep blue-colored prismatic crystals. Yield: 4 mg; 2.1%. IR, ν, cm⁻¹: 2957 m, 2891 m, 2851 m, 2806 m, 2269 vw, 2254 w, 2241 m, 1520 s, 1498 s, 1446 m, 1406 m, 1343 s, 1322 s, 1248 m, 1219 m, 1176 m, 1121 w, 1055 m, 977 w, 949 m, 929 m, 824 m, 805 s, 765 m, 681 w, 658 m, 538 w, 515 w. Crystal data for **[TMPD][TCBT]**: $C_{10}H_8N_6$, M = 212.22, monoclinic, space group $P2_1/a$, a = 7.3864(3) Å, b = 15.0865(3) Å, c = 9.4932(4) Å, β = 95.2112(14)°, V = 1053.50(6) Å³, Z = 4, ρ_{calcd} = 1.338 Mg/m³, absorption coefficient = 0.090 mm⁻¹, F(000) = 440, reflections collected = 4380, independent reflections = 2381 [R(int) = 0.0237], GOF = 1.050, R = 0.0406, wR_2 = 0.0990. CCDC-178429.

Supporting Information Available: X-ray CIF files for [TTF][TCT], [HTMPD]⁺[DCTO]⁻, {[Cr(mes)₂]⁺}₂[TCT]₂²⁻·2MeCN, and [TMPD][TCBT] (these files have also been deposited with the Cambridge Crystallographic Data Centre, ref nos. CCDC-172417, CCDC-172418, CCDC-163649, and CCDC-178429, respectively) and computational data for 1,3,5-tricyanotriazine, the 1,3,5-tricyanotriazine anion, the 1,3,5-tricyanotriazine dianion, 4,4′,6,6′-tetracyano-2,2′-bitriazine, the 4,4′,6,6′-tetracyano-2,2′-bitriazine anion, and the 2,4-dicyano-6-hydroxy-s-triazine anion, [DCTO]⁻. This material is available free of charge via the Internet at http://pubs.acs.org.

JO025833H